

Supporting Information

An anthracene based conjugated triazine framework as a luminescent probe for selective sensing of p-nitroaniline and Fe(III) ions

Haitao Hong,^{‡a,b} Ni Wu,^{‡a} Mingxi Han,^a Zhiyong Guo,^{*a} Hongbing Zhan,^a Shaowu Du,^b Banglin Chen^{*c}

^aCollege of Materials Science and Engineering, Fuzhou University, Fuzhou 350108, Fujian, P.R China.

^bFujian Key Laboratory of Functional Marine Sensing Materials, Minjiang University, Fuzhou 350121, Fujian, P.R China.

^cDepartment of Chemistry, University of Texas at San Antonio, One UTSA Circle, San Antonio, TX 78249-0698, USA.

E-mail: guozhy@fzu.edu.cn (Z.G.), banglin.chen@utsa.edu (B.C.).

Experimental Section

Chemicals and instrumentation: All chemical reagents and solvents were purchased from commercial suppliers and used as received. The ^1H NMR and solid-state cross-polarization magic angle spinning (CP/MAS) ^{13}C NMR spectra were recorded at 298 K using Bruker Advance III 500 MHz spectrometer. The PXRD data were collected on a Rigaku Ultima III X-ray diffractometer using Cu-K α radiation at 35 kV and 30 mA. Thermogravimetric Analysis (TGA) was performed on a NETZSCH STA449-F5 thermogravimetric analyzer. The sample was heated from 50 °C to 800 °C at a rate of 10 °C/min under an N $_2$ atmosphere. Fourier-transform infrared spectroscopy (FTIR) was performed on a Nicolet 5700 spectrometer. Gas adsorption isotherms were collected using a Micromeritics ASAP 2020 plus surface area and porosity analyzer after the samples had been degassed at 100 °C for 10 h under vacuum. The obtained adsorption-desorption isotherms were evaluated to give the pore parameters, including Brunauer-Emmett-Teller (BET) and Langmuir specific surface area (SA_{BET} and SA_{Lang}), pore size, and pore volume. The pore size distribution was calculated from the adsorption branch with the nonlocal density function theory (NLDFT) approach. The Luminescence excitation and emission spectra were conducted on an FLS1000 Series of Fluorescence Spectrometers at room temperature utilizing a 450 W xenon lamp as an excitation source. The slit widths of excitation and emission were set the same in each sensing experiment.

Limit of detection (LOD) Calculation:

Limit of detection was determined according to the following definitions:

$$S_b = \sqrt{\frac{\sum_{i=1}^n (x_i - \bar{x})^2}{n-1}} \quad (1)$$

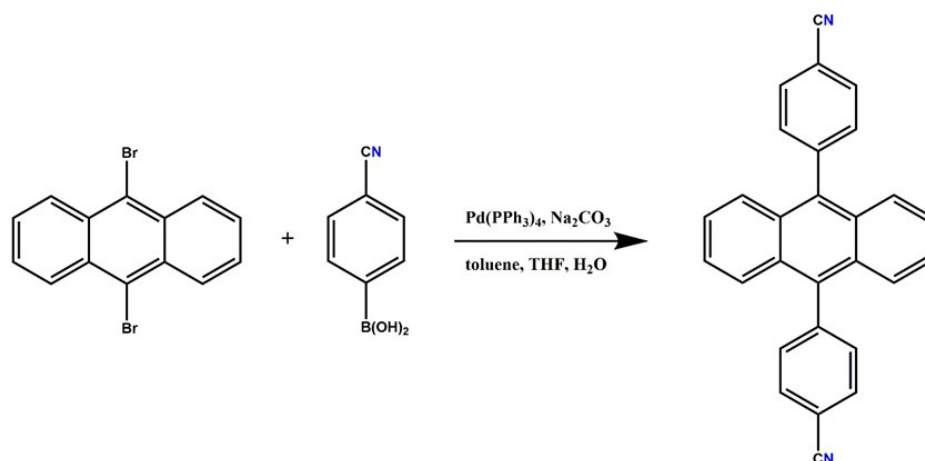
$$S = \frac{\Delta I}{\Delta c} \quad (2)$$

$$LOD = \frac{3S_b}{S} \quad (3)$$

Firstly, the standard deviation (S_b) was calculated by measuring the fluorescence intensity of probe molecule in ethanol for 11 times and then got the average intensity (\bar{x}). By fitting the data into equation (1), the value of standard deviation (S_b) was obtained. Secondly, a certain amount of the analyte was added into the solvent and the resulting variation of the intensity (ΔI) was recorded. By fitting the data into equation (2), where is the variation of intensity, and Δc is the variation of quencher concentration, the value of precision S was calculated. Finally, the LOD was calculated according to Function (3).

Synthesis of the 9,10-Bis(4-cyanophenyl)anthracene (DPA): The 9,10-Bis(4-cyanophenyl)anthracene was prepared by following the procedure described in the literature.¹ A mixture of 9,10-dibromoanthracene (2.12 g, 6.3 mmol), 4-cyanophenylboronic acid (2.39 g, 16.25 mmol), Pd(PPh₃)₄ (0.728 g, 10 mol%), Na₂CO₃ (230 mg, 2.1 mmol) in H₂O (10 mL) and solvent of THF (45 mL) and toluene (45 mL) was heated at 85 °C under N₂ for 8 h. After the reaction (TLC monitoring), the mixture was diluted with H₂O and extracted with Et₂O. The combined organic

layers were washed with H₂O, brine and dried (MgSO₄). The solvent was evaporated and the crude product left was charged on a silica gel column. Elution of the column with 4% EtOAc-petroleum ether gave the desired cross-coupling product (1.56 g, 65%) as a white crystalline solid. IR (KBr): 2229 (C≡N), 2163 cm⁻¹. ¹H NMR (300



MHz, CDCl₃): δ = 7.41-7.43 (m, 4 H, ArH), 7.57-7.59(m, 4 H, ArH), 7.63 (d, J = 8.2 Hz, 4 H, ArH), 7.95 (d, J = 8.2 Hz, 4 H, ArH).

Scheme S1. Synthetic routes for 9,10-Bis(4-cyanophenyl)anthracene (DPA).

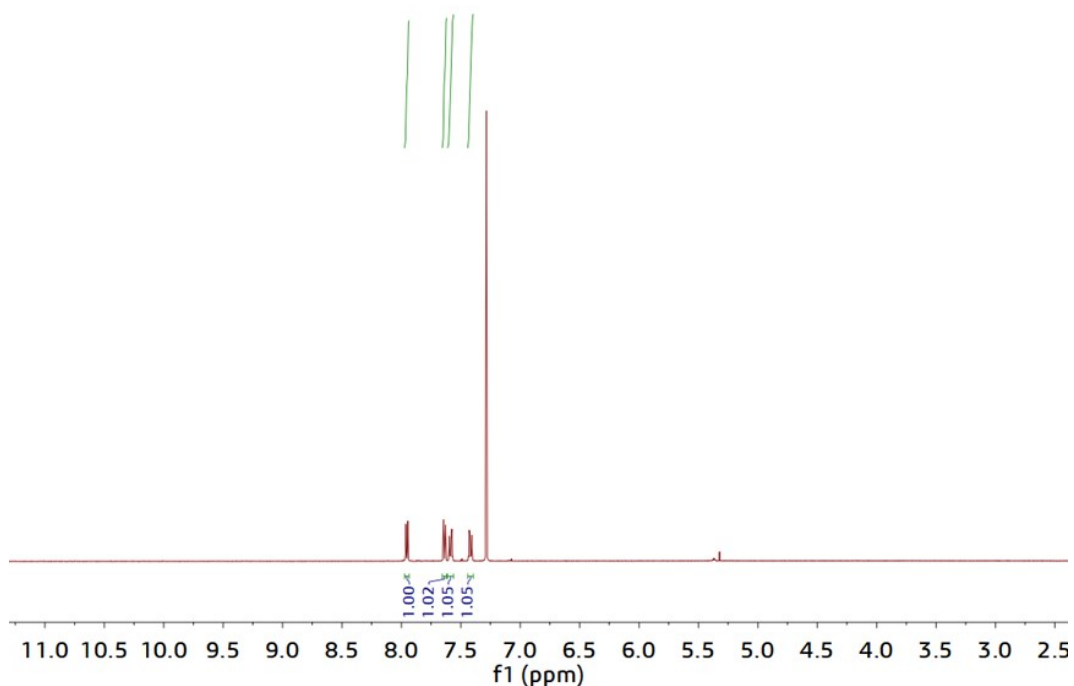


Figure S1. ^1H NMR spectrum of 9,10-Bis(4-cyanophenyl) anthracene (DPA).

General Characterization of DPA-CTF:

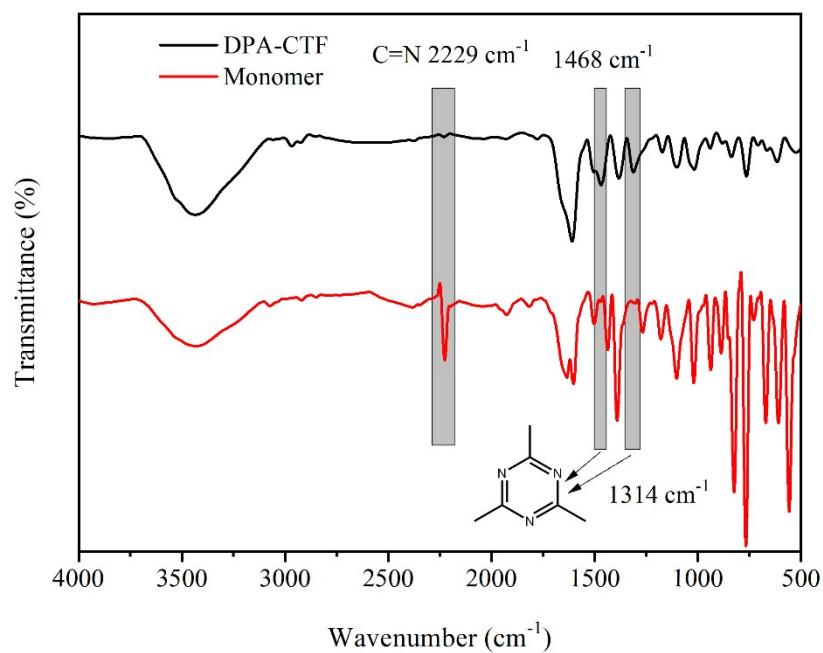


Figure S2. Fourier transform infrared (FT-IR) spectra of the monomer (DPA) and the polymer (DPA-CTF).

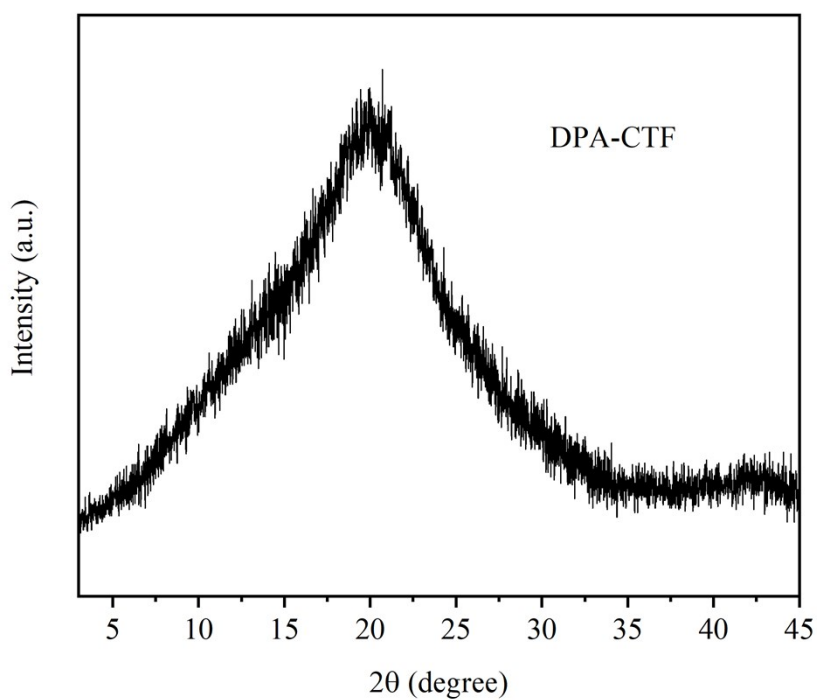


Figure S3. Powder XRD patterns of DPA-CTF

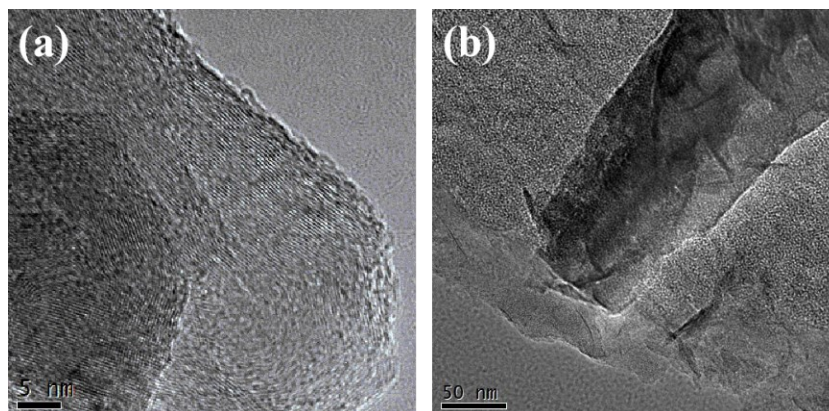


Figure S4. TEM pictures of DPA-CTF: a and b.

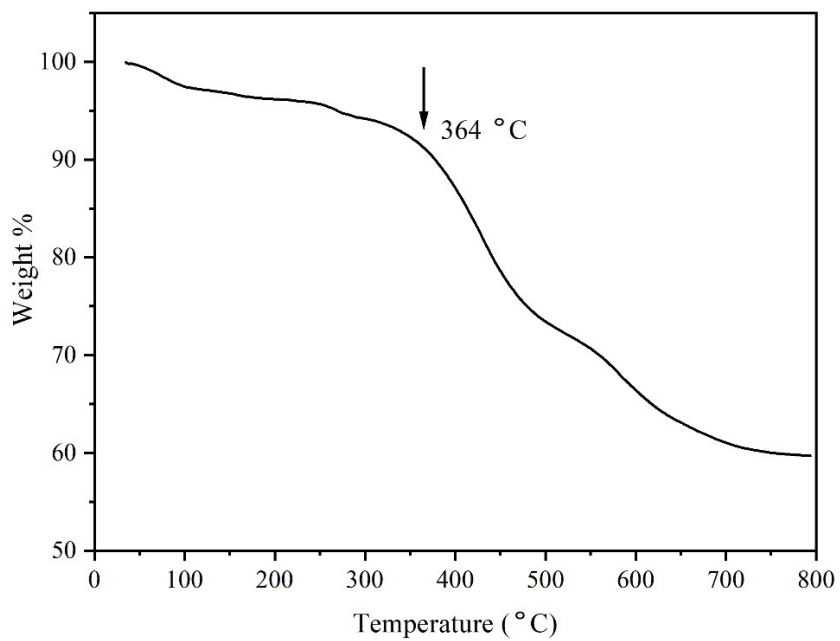


Figure S5. TGA curve of DPA-CTF under nitrogen condition.

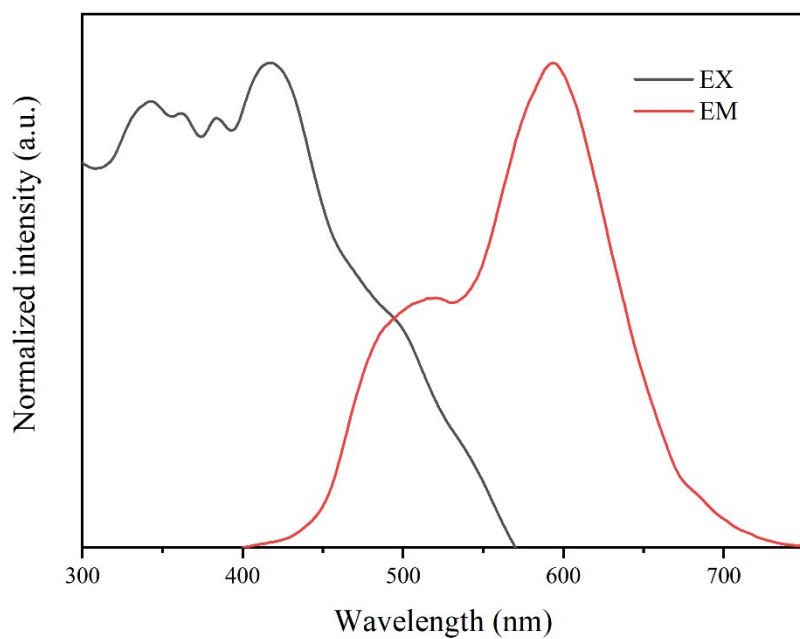


Figure S6. The fluorescence spectra of DPA-CTF in the solid state excited in 527 nm and the emission peaks at 640 nm.

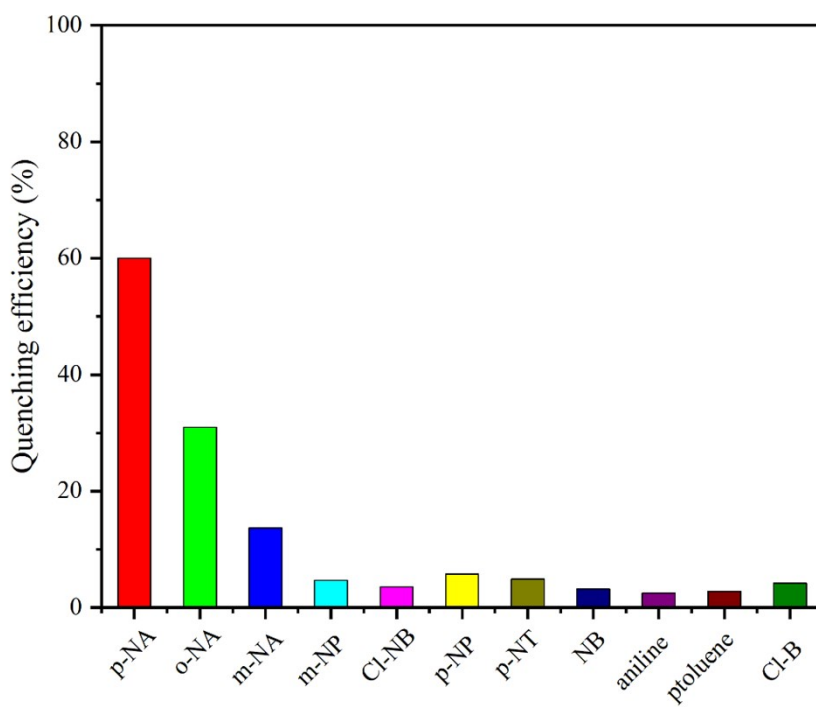


Figure S7. Quenching efficiencies of DPA-CTF with addition the same amount (0.05

mM) of different aromatic compounds.

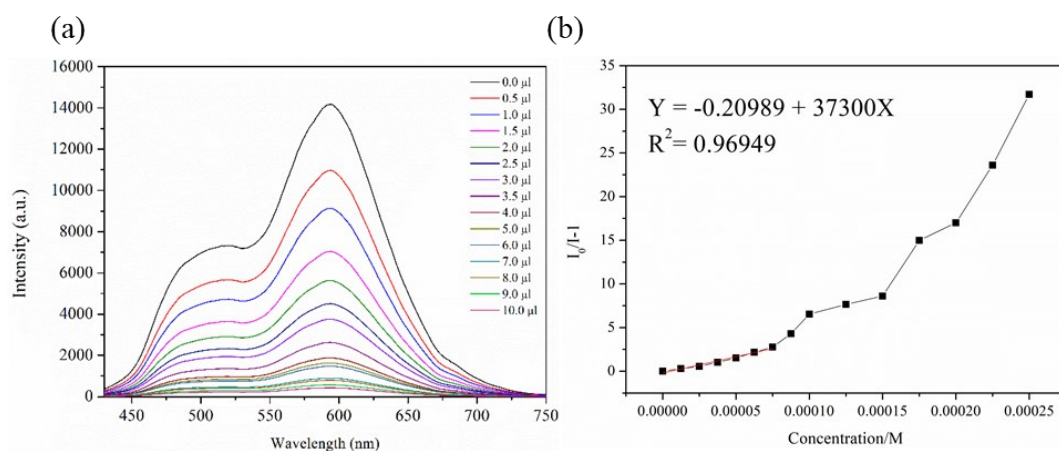


Figure S8. (a) Fluorescence titration spectra of DPA-CTF in ethanol solution ($0.1 \text{ mg} \cdot \text{mL}^{-1}$, upon addition of p-NA ($\lambda_{\text{ex}} = 418 \text{ nm}$); (b) The relationship of I_0/I_e with different concentration of p-NA.

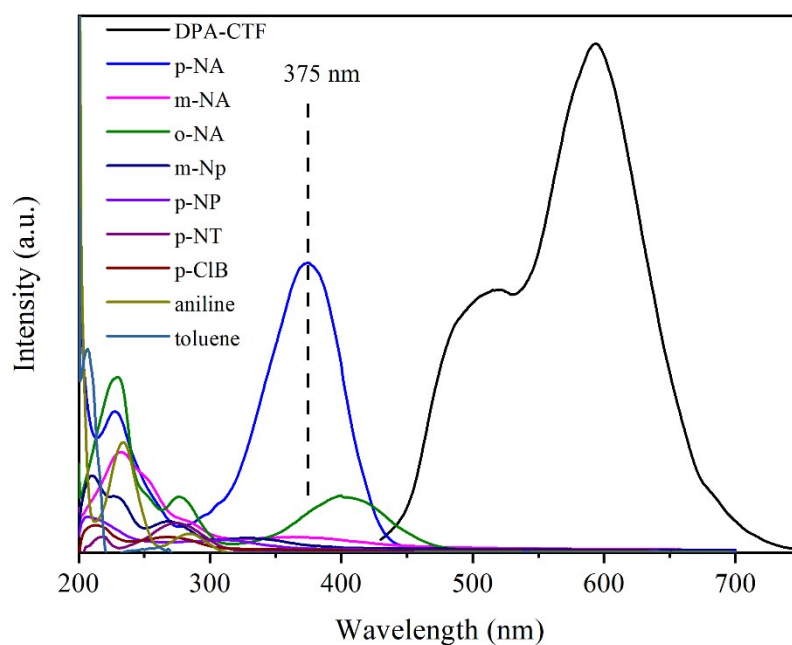


Figure S9. Spectra overlap between the absorption spectra of aromatic analytes ($5 \times 10^{-4} \text{ M}$) and the emission spectrum of DPA-CTF in ethanol solution.

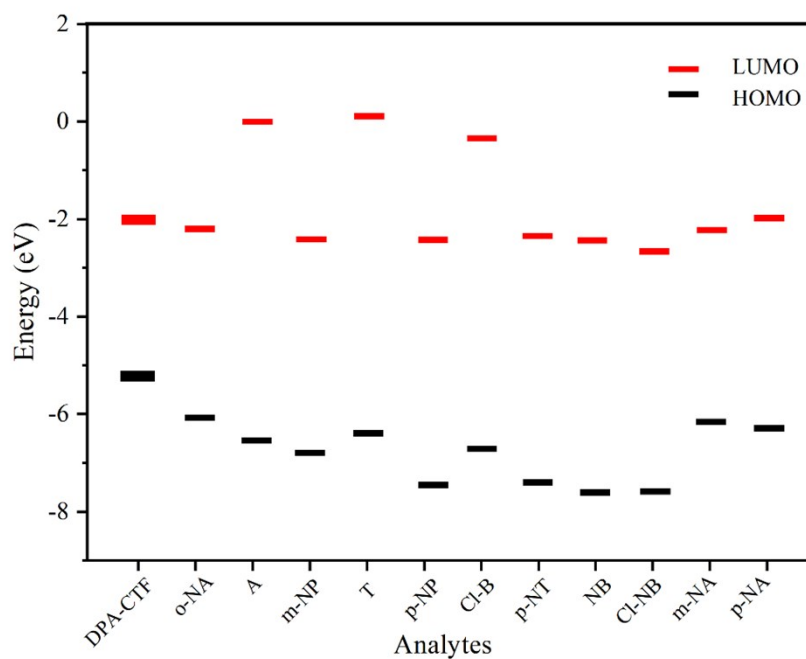


Figure S10. HOMO and LUMO energy levels calculated for DPA-CTF and different aromatic analytes.

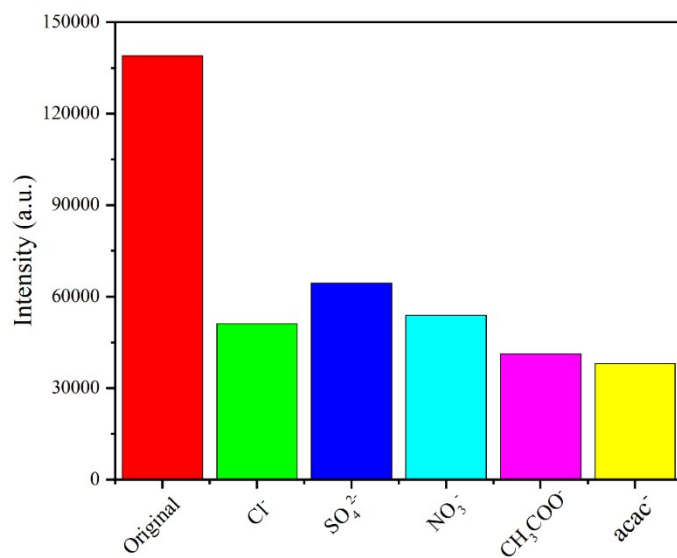


Figure S11. The maximum emission intensity of DPA-CTF shows the counterion effects in the metal ion sensing experiments. The concentration of different Fe³⁺ salts in ethanol suspensions is 0.5 mM ($\lambda_{\text{ex}} = 418$ nm). Fe(acac)₃ refers to ferric acetylacetonate.

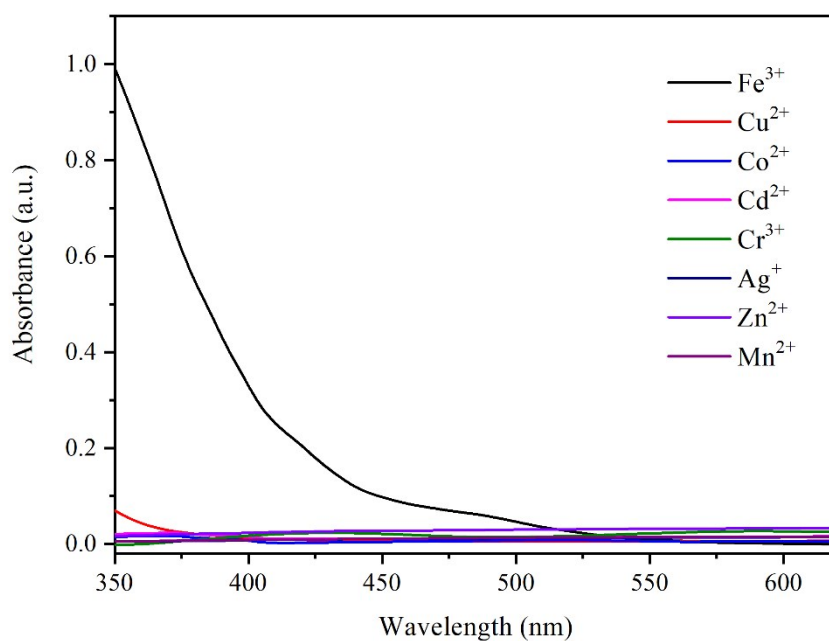


Figure S12. UV-Vis spectra with the same condensation (1×10^{-4} M) of $M(\text{NO}_3)_x$ ($M = \text{Fe}^{3+}, \text{Cu}^{2+}, \text{Co}^{2+}, \text{Cd}^{2+}, \text{Cr}^{3+}, \text{Ag}^+, \text{Zn}^{2+}$ and Mn^{2+}) in ethanol solution.

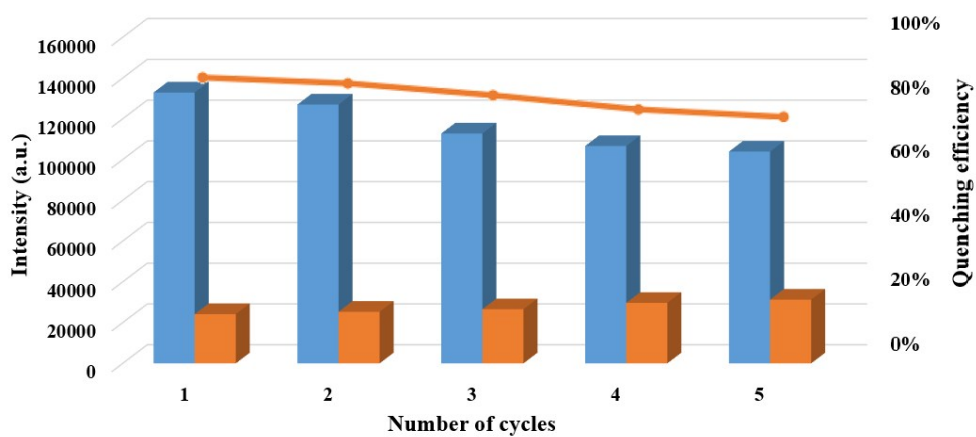


Figure S13. Reproducibility of the quenching ability of DPA-CTF dispersed in ethanol solution and in the presence of 1×10^{-4} M p-NA.

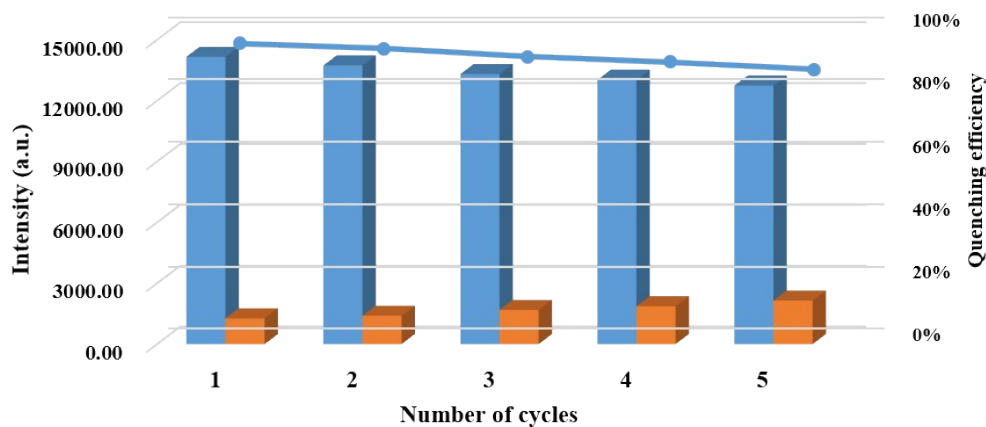


Figure S14. Reproducibility of the quenching ability of DPA-CTF dispersed in ethanol solution and in the presence of 0.5 mM Fe(NO₃)₃.

Table S1. A comparative account of nitroaniline detection by fluorescent porous materials.

Material	$K_{sv}(M^{-1})$	LOD (M)	Reference
W-N-CDs	8.82×10^3	1×10^{-6}	2
PBPMCz	2.2×10^4	1.1×10^{-6}	3
PTPTB	7.08×10^4	4.2×10^{-6}	4
TMU-4S	3.0×10^4	5×10^{-5}	5
TPDC-DB	1.7×10^4	3.3×10^{-6}	6
[Cd(dpa)(pta)]·nDMF	6.26×10^3	7.4×10^{-7}	7
[Ba(PSTP)0.5(H ₂ O)] _n	5.4×10^5	3.1×10^{-7}	8
DPA-CTF	3.7×10^4	1.5×10^{-6}	This work

Supporting References

- 1 S. Kotha, A. K. Ghosh and K. D. Deodhar, Synthesis of symmetrical and unsymmetrical 9,10-diarylanthracene derivatives via bis-Suzuki-Miyaura cross-coupling reaction, *Synthesis-Stuttgart*, 2004, **4**, 549-557.
- 2 H. Yuan, D. Li, Y. Liu, X. Xu and C. Xiong, Nitrogen-doped carbon dots from plant cytoplasm as selective and sensitive fluorescent probes for detecting p-nitroaniline in both aqueous and soil systems, *Analyst*, 2015, **140**, 1428-1431.
- 3 L. Qian, H. Hong, M. Han, C. Xu, S. Wang, Z. Guo and D. Yan, A ketone-functionalized carbazolic porous organic framework for sensitive fluorometric determination of p-nitroaniline, *Microchim. Acta*, 2019, **186**, 457.
- 4 F. Wei, X. Cai, J. Nie, F. Wang, C. Lu, G. Yang, Z. Chen, C. Ma and Y. Zhang, A 1,2,3-triazolyl based conjugated microporous polymer for sensitive detection of p-nitroaniline and Au nanoparticle immobilization, *Polym. Chem.*, 2018, **9**, 3832-3839.
- 5 M. Bagheri, M. Y. Masoomi and A. Morsali, Highly sensitive and selective ratiometric fluorescent metal-organic framework sensor to nitroaniline in presence of nitroaromatic compounds and VOCs, *Sens. Actuators B Chem.*, 2017, **243**, 353-360.
- 6 A. Deshmukh, S. Bandyopadhyay, A. James and A. Patra, Trace level detection of nitroanilines using a solution processable fluorescent porous organic polymer, *J. Mater. Chem. C*, 2016, **4**, 4427-4433.
- 7 J.-H. Wang, G.-Y. Li, X.-J. Liu, R. Feng, H.-J. Zhang, S.-Y. Zhang and Y.-H. Zhang, A fluorescent anthracene-based metal-organic framework for highly selective detection of nitroanilines, *Inorg. Chim. Acta.*, 2018, **473**, 70-74.
- 8 Y. Sun, B. X. Dong and W. L. Liu, Construction of a new three-dimensional fluorescent probe based on Ba-II ions and 2,5-bis-(4-carboxy-phenyl)sulfanye-terephthalic acid, *J. Solid State Chem.*, 2019, **278**, 7.